

Modeling of Electrothermal Flow Mixing in Lab on Chip Microfluidic Devices

Vishaka Wasnik

A Dissertation Submitted to
Indian Institute of Technology Hyderabad
In Partial Fulfillment of the Requirements for
The Degree of Master of Technology



भारतीय प्रौद्योगिकी संस्थान हैदराबाद
Indian Institute of Technology Hyderabad

Department of Biomedical Engineering

June, 2016

Declaration

I declare that this written submission represents my ideas in my own words, and where others' ideas or words have been included, I have adequately cited and referenced the original sources. I also declare that I have adhered to all principles of academic honesty and integrity and have not misrepresented or fabricated or falsified any idea/data/fact/source in my submission. I understand that any violation of the above will be a cause for disciplinary action by the Institute and can also evoke penal action from the sources that have thus not been properly cited, or from whom proper permission has not been taken when needed.



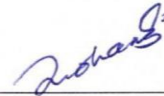
(Signature)

Vishaka Wasnik
(Student Name)

BM14MTECH11010
(Roll No)

Approval Sheet

This thesis entitled “Modeling of Electrothermal Flow Mixing in Lab on Chip Microfluidic Devices” by Vishaka Wasnik is approved for the degree of Master of Technology from IIT Hyderabad.



Dr. Jyoti Ranjan Mohanty
Assistant Professor
Department of Physics
Indian Institute of Technology, Hyderabad
Examiner



Dr. Jyotsnendu Giri
Assistant Professor
Department of Biomedical Engineering
Indian Institute of Technology, Hyderabad
Examiner



Dr. Harikrishnan Narayanan Unni
Assistant Professor
Department of Biomedical Engineering
Indian Institute of Technology, Hyderabad
Adviser

Acknowledgements

I express my sincere gratitude to supervisor, respected Dr. Harikrishnan Narayanan Unni, under whose esteemed guidance and supervision, this work has been completed. This project work would have been impossible to carry out without his motivation and support throughout.

I am grateful to the Micro-Fluidic laboratory Of the Department of Biomedical Engineering, IIT Hyderabad for providing the computational facility to carry out the modeling part of the project work

Dedicated to

This thesis is dedicated to my beloved parents,
for their endless love, support, encouragement and trust.

Thank you both of you for giving me strength to reach for the star and chase my dreams. Also, this thesis is dedicated to my teachers, for their constant support and motivation. Thank you for your guidance and encouragement throughout the study.

And to all my friends.

Abstract

Electrokinetics involves the study of liquid or particle motion under the action of an electric field; it includes electroosmosis, electrophoresis, dielectrophoresis, and electrowetting, etc. AC Electrokinetics (ACEK) has attracted much research interest for microfluidic manipulation for the last few years. It shows great potential for functions such as micropumping, mixing and concentrating particles. Based upon the actuation pattern microfluidic- based mixing devices can be categorized in two types. They are passive mixing microfluidic device and active mixing microfluidic device. Passive mixers typically utilize geometrical advantages to enhance mixing and they do not require external forces but a long mixing path was required. Active mixers are generally more effective than passive mixers. They utilize external driving forces like acoustics vibrations, electric and magnetic instability, temperature gradient due to joule heating etc. Like AC electroosmosis (ACEO) phenomena, AC electrothermal (ACET) effect is a hydrodynamic phenomena and acts on a suspended particle only through fluid drag because of Joule Heating. The challenges with ETE devices are the deciding threshold voltage, used for clinical diagnostic to protect the cell from damage, choosing conductivity of the fluid, Electrode patterning and the switching of the electrode.

In this thesis, the design parameters, voltage and frequency actuation pattern of electrodes is obtained by trial and error method to obtain the chaotic flow field to enhance the mixing efficiency. Firstly, 2D simulation is carried out over a rectangular channel with microelectrodes located at sidewalls to observe the mixing behavior with different voltage actuation pattern between adjacent electrodes, with different concentration of fluid, deciding the appropriate channel dimensions. Secondly, the effectiveness of several parameters were observed by 3D simulation for further enhancement of fluid mixing, including AC electric field frequency, applied voltage, conductivity of fluid, AC signal phase shift between the electrodes etc.

Nomenclature

Symbol	Definition
σ	Fluid conductivity
μ_+	Ion conductivity for cation
μ_-	Ion conductivity for anion
c	Concentration
ρ_m	Mass density
p	Pressure
∇	Surface gradient operator
C_p	Heat capacity
\bar{v}	Fluid velocity
K	Thermal conductivity
ρ_q	Volume charge density
t	Time scale
D	Diffusivity
τ	Charge relaxation time
f_c	Crossover frequency

Contents

Declaration.....	ii
Approval Sheet	iii
Acknowledgements.....	iv
Abstract.....	vi
Nomenclature	vii
1 Introduction	1
1.1 General.....	1
1.2 An Introduction to Electrokinetics	2
2 Literature Review	4
2.1 Objective and Scope	6
3 Theory	7
3.1 Introduction.....	7
3.2 AC Electrothermal (ACET) effect in Microfluidics	7
4 Modeling	11
4.1 Geometry (2-D).....	11
4.2 Geometry (3-D).....	12
4.3 Flow pattern and Boundary condition.....	13
4.3.1 Laminar flow	14
4.3.2 Heat transfer in fluid.....	14
4.3.3 Transport of diluted species.....	14
4.4 Temperature dependent properties.....	14
4.5 Parameter and Meshing.....	15
4.6 Electrode Actuation Pattern	17
5 Results and Discussions	19
5.1 2D Simulation	19
5.2 3D Simulation	25
Conclusion	32
References	32

Chapter 1

Introduction

1.1 General

Lab-On a chip or Loc is a technology that integrates microfluidic system on miniature chip which can perform micrototal and/or chemical analysis [3]. A Lab-on-a-chip can contain mixers, reservoirs, pumps, valves, reactor, separator, and other components to manipulate buffer fluids or cells. Providing the advantages like rapid analysis, low reagents consumption, less chemical waste production, high throughput with less cost and a significant improvement in performance. These devices are normally portable and disposable after use

Mixing of two or more fluids is one of the key operations for LOC devices where rapid mixing of reagent/reactants is often required. For example in many biological processes, such as enzyme reaction, protein folding, DNA purification, etc. it is important to achieve a homogenized solution of the analytes. In microfluidics, the nature of flow is Laminar (or “creeping flow to be precise), thus the mixing is extremely slow and depends solely on molecular diffusion. Therefore, there is a need for developing new technique to enhance mixing of different concentration reagents in diffusion dominated processes inside the microchannels. Recent years have witnessed tremendous advances in Electrokinetic mixing in microfluidics. Electrokinetic (EK) method is based on Electric Field driven flows, where mechanical flow control components such as valves are mostly eliminated. An introduction to Electrokinetics is provided in the following section.

1.2 Introduction to Electrokinetics

The term ‘Electrokinetics’ refers to motion of liquids or particles under the influence of external electric field. It includes Electroosmosis, Electrophoresis, Dielectrophoresis, electrowetting etc. used for applications like mixing two or more analytes , pumping of fluids, sorting of cells, detection and concentration [9]. Electrokinetic mixing is subdivided into two categories i.e. Passive mixing and Active mixing.

Passive mixing refers to the mixing systems which make use of geometry topologies, surface properties of microchannels. It does not require any external driving force to enhance mixing effect in electrokinetically driven system. For example, laminated surfaces can be employed for chaotic mixing in T- or Y- shaped microchannels, where flow diversion aids the mixing of analytes that can only mix via diffusion otherwise [33].

Active mixings refers to the mixing systems which require external driving force to enhance it. The external force can be time-dependent or independent electrical force, acoustic force, magnetic force, EK time- pulsed, EK instability [11], thermal force due to joule heating [9] etc. Therefore, the challenge in designing an active electrokinetic micro-mixer is the selection of operation conditions, the choice of driving amplitudes of DC and/or AC frequencies considering geometry of micro-mixer.

Traditional electrokinetic mixing systems apply high dc voltages across the microchannel, this generates bubble and pH gradients from electrochemical reactions. To minimize this adverse effects low voltage AC electro-osmotic (EO) mixing has been studied [18-19]. However, Electro-osmotic mixing is not effective at high fluid conductivity. It mainly depends on the electrical double layer (EDL) thickness. EDL thickness is in dependent on ionic concentration and higher ionic concentration results in reduction of EDL thickness [14-16]. AC electrothermal (ACET) effect can be used for mixing biofluids of high conductivity (>0.1). ACET is based on temperature gradient due to Joule heating when fluid is under action of electric field [29].

In the present study, we focus mainly on AC electrothermal (ACET) mixing, focusing on the underlying physical mechanisms for enhancement of mixing efficiency. The effect of electrode actuation pattern, frequency, driving amplitudes with different fluid conductivities are studied in detail to ascertain the effect on the micro-mixer efficiency. The above-

mentioned study has been performed by coupled field modeling via COMSOL Multiphysics.

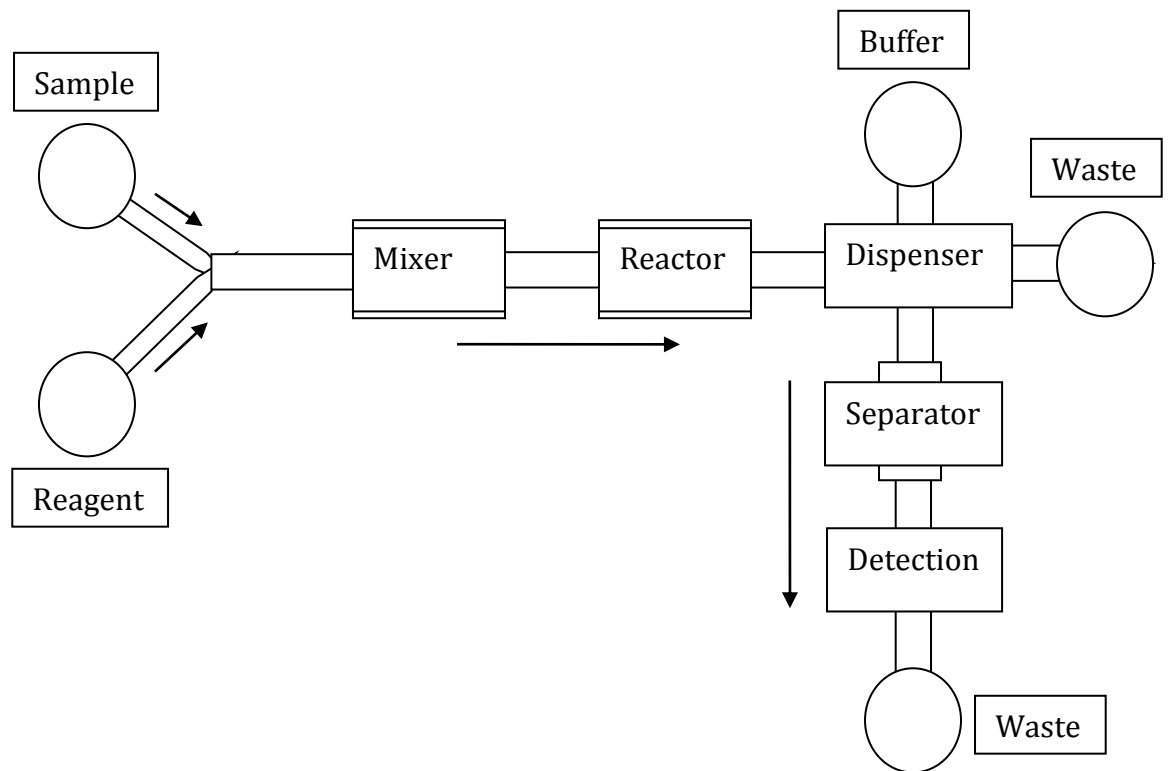


Fig.1) Illustration of microfluidic components in a typical Lab-on-chip device

Chapter 2

Literature Review

T J. Cao, P. Cheng, F.J.Hong [10], reported 2D numerical investigation of AC electrothermal vortex enhanced micromixer. The FEM method was used to investigate mixing efficiency of sample in a KCL solution. The microchannel with a height of $W=50\ \mu\text{m}$, length $L=200\ \mu\text{m}$ and a pair of electrodes ($10\ \mu\text{m}$ size) with gap of $10\ \mu\text{m}$ in between them was used. The simulation results show that the mixing efficiency of two fluids with concentrations of 0 and $1\ \text{mol}/\text{m}^3$ increases from 17.4 to 33.3% at the end of microchannel, when the electrodes are actuated with 10 and -10V at an AC frequency of 1MHz. It is found that the electrothermal flow effect, in the frequency range (0.1 to 10 MHz) for which Coulomb force is predominant. And it induces vortex flow motion near to the electrode corner ends thus causing stirring the flow stream and enhancing its mixing efficiency. Furthermore, by using two pairs of electrodes on opposite side walls at optimal position, with same actuation, the mixing efficiency increases to 49.6%. It was noted that the mixing efficiency decreases when the actuating frequency is higher than 10MHz. this is because of decrease of Coulomb force at higher frequencies. For $L=700\ \mu\text{m}$ microchannel length with 16 pairs of electrodes on the walls and voltage of 10 Vrms in AC frequency range of 0.1-10MHz is applied. The numerical results show that the mixing efficiency of 98% is achieved at the end of the microchannel.

Chieh-Li Chen, Her-Terng Yau, Ching- Chang Cho and Cha'o-Kuang Chen [5] reported enhancement of microfluidic mixing using Harmonic and chaotic electric field. They put forward a computational proposition that, mixing efficiency is changeable and irregular under the aperiodic excitation generated by chaotic electric potentials. It was shown that, the mixing efficiency can be improved when using harmonic electric field as well as with suitably oscillating chaotic electric potentials with a higher power spectral density.

Hope C. Feldman, Marin Sigurdson and Carl D. Meinhart [6] has investigated Electrothermal flow stirring to enhance the temporal performance of heterogeneous

immuno-sensor in microfluidic systems, in which it provides more binding opportunities between suspended antigens and wall-immobilized antibodies. In the experiment, a biotin-streptavidin heterogeneous assay is observed in which biotin is immobilized, and fluorescently-labeled streptavidin is suspended in a high conductivity buffer ($\sigma=1$ s/m). Microelectrodes of microwell were driven at frequency of $f=200$ kHz and $10V_{rms}$. Fluorescent intensity measurements show that, electrothermal stirring increases the binding rate by a factor of almost nine, for a five minute assay. Similar binding improvement was measured for longer assays, up to fifteen minutes. The above mentioned experimental study established the potential of electrothermal flow technique as a means for mixing in biochips.

Chih-Kai Yang, Jeng-Shian Chang, Sheng D. Chao, and Kuang-Chong Wu [12], worked on the modeling of two dimensional simulations on immunoassay for biosensor, in which electrothermal effect induces the stirring flow and enhances the transport rate of analytes. They performed finite-element simulations of electrothermal effect on the reaction kinetics of C-reactive protein (CRP)-anti-CRP. The two dimensional geometry includes microchannel of $500 \times 150 \mu m^2$ containing a reacting surface of $40 \times 3 \mu m^2$ in the middle of the bottom side and a pair of electrodes on the top opposite to the reacting surface. The buffer solution mixed with analytes flows from left to right. The ligands were immobilized on the reacting surface. For diffusion limited proteins, the diffusion boundary layer on the reacting surface hinders the binding reaction. By varying the position of reacting surface i.e. by varying the distance between electrode and reacting surface, different interference pattern of vortices are observed at each locations. Thereby, observing reduction of the thickness of diffusion boundary layer on the reacting surface. These patterns are utilized to optimize the enhancement factor, yielding 5.166 and 3.744 times for association and dissociation, respectively, under voltage of $15 V_{rms}$ and frequency of 100 kHz.

S Loire, P Kauffmann, I Mezić and C D Meinhart [2], discusses theoretical and experimental study of ac electrothermal flows. They developed a full enhanced model using electrical thermal coupling and temperature dependent expressions for electrical conductivity and dynamic viscosity for rise in temperature. They demonstrated that for high temperature elevation, electrothermal coupling cannot be neglected and buoyancy force effect has to be taken into account. They performed microparticle- image velocimetry (μ PIV) measurements to evaluate the full enhanced model. Furthermore, the importance of

the competition between ACET and buoyancy driven convective flow at low voltages was observed experimentally and theoretically.

A. Eden, M. Sigurdson, C. D. Meinhart, I. Mezić [4], introduced a hybrid experimental-numerical method for generation of 3D flow information from 2D particle image velocimetry(PIV) experiment data and finite element simulations. This method is applied to an alternating current electrothermal(ACET) micromixer in conjunction with 2D PIV data to estimate 3D steady state flow condition. The optimization algorithm reduced the normalized root mean square error (NRMSE) between the simulated velocity field and experimental fields in the target region by more than an order of magnitude. This method shows promise in developing simulations that can more accurately reflect experimental conditions, and has potential applications in modeling flow measurement systems where the dominant physical effects are well characterized and understood.

2.1 Objective and Scope

The objective and challenges of this project are as follows:

- To develop 2D/3D geometrical models depicting microchannel and embedded microelectrode arrays
- To model associated phenomenological equations using proper geometry meshing
- To study the effect of actuation voltage and electrode switching pattern on flow velocity, temperature and concentration fields.
- To study the ACET mixing of two fluids when introduced with different concentrations

The Scope of this project are:

- It has no moving parts therefore it is easy to fabricate using micro/nano fabrication technology
- Numerous chemical and biological experiments can perform on the same platform, reducing the reagent volumes from liters to nano liters. Reactions happen much faster in a small scale and thus leading to easy manipulation of cells and particles like focusing, trapping and mixing.
- The AC signal avoids splitting of water molecules ie electrolysis.
- Biochemical analysis frequently involves samples with high conductivities ie in 0.02-1 s/m range. ACET was found effective for high conductive fluids.

Chapter 3

Theory

3.1 Introduction

Microfluidics lab-on-chip devices (Microchips) are an alternative to conventional biochemical laboratories, and are revolutionizing many application, such as molecular biology procedures, DNA analysis, proteomics (the study of proteins) and clinical pathology (diagnostic of diseases) [3]. They are becoming increasingly complex, with thousands of components, but are designed manually (called bottom-up full-custom design), which is extremely labor intensive and error prone.

The challenges facing microchips are similar to those faced by microelectronics some decades ago. A typical microprocessor today has over a billion transistors. Such a design complexity is possible because engineers are using Computer-Aided Design (CAD) tools, which, starting from a specification of the desired functionality, automatically build the best possible design (such a process is called top-down design). As in the microelectronics area, COMSOL tools will reduce the development costs, increase the design productivity and yield, and are the key to the further growth and market penetration of microchips. My research vision is to develop a design flow for microchips, which, starting from a system specification can automatically derive a physical microchip design.

3.2 AC Electrothermal (ACET) effect in Microfluidics

ACET effect arises from uneven Joule heating due to an electric current flowing through the fluid. The theoretical foundation of ACET mechanism is a coupling problem which involves electric, thermal and fluidic mechanical formulations. At the time an ac signal is applied, the electric field is established within the solution. Charged particles are attracted by the electrode with opposite polarity and migrate, which forms the ionic current. The current density in the fluid is expressed as [37]:

$$j = \sigma E = (\mu_+ + \mu_-)cE \dots\dots\dots(1)$$

Where, σ is the fluid conductivity, c is the concentration, (μ_+) and (μ_-) is the limiting ion conductivity for anions and cations which are constants at 298K.

Equation (1) indicates the resistive manner of fluid bulk. In addition, the electrical Reynolds number is much less than one in microfluidic systems, implying that ohmic current dominates.

The current flows through the ohmic fluid bulk and henceforward generates heat (this process is named the Joule heating). In order to estimate the temperature rise in micro-electrode devices, the energy balance equation given below is used to link the electric and thermal field together [30]

$$\rho_m c_p \bar{v} \cdot \nabla T + \rho_m c_p \frac{\partial T}{\partial t} = k \nabla^2 T + \sigma E^2 \dots\dots\dots(2)$$

Where ρ_m is the mass density, c_p is the heat capacity, \bar{v} is the fluid velocity and k is the thermal conductivity. The first term in Equation (2) illustrates the effect of heat convection by fluid motion. The effect of fluid motion on the temperature profile is assumed to be minimal, the effect of fluid flow on the temperature profile can be neglected even for a fluid velocity approaching 1mm/s.

The second term in Equation (2) stands for the temperature diffusion process. The diffusion time is typically at the order of 10^{-3} s in micro-systems. In another words, the thermal equilibrium is established within 10^{-3} s after applying the signal. Thus, for the fields of frequency greater than 1 kHz, the differential temperature change is neglected [30] Therefore the Equation (2) is reduced to

$$k \nabla^2 T + \sigma E^2 = 0 \dots\dots\dots(3)$$

The temperature rise is estimated by substituting for the electric field as [30]:

$$\Delta T \approx \frac{\sigma V_{rms}^2}{k} \dots\dots\dots(4)$$

Since the electric field is highly non-uniform, the power density is also highly non-uniform. The temperature variation in fluid gives rise to local changes in permittivity and conductivity. These inhomogeneities in fluid permittivity and conductivity lead to the net force in fluid. The general expression for the electrical force per unit volume is given as [30]:

$$f_E = \rho_q E - \frac{1}{2} E^2 \nabla \varepsilon + \frac{1}{2} \nabla \left(\rho_m \frac{\partial \varepsilon}{\partial \rho_m} E^2 \right) \dots\dots\dots(5)$$

Where ρ_q is the volume charge density. The last term is the electrostriction force that can be ignored in an incompressible fluid (it is the gradient of a scalar). The first term is the Coulomb force, and the second is the dielectric force. The estimation of these forces can be made from the charge density equation as described in Gauss's law $\rho_q = \nabla \cdot (\varepsilon E)$

By performing a lowest order perturbative expansion and separating electric field into the sum of the applied field E_0 and the perturbation field E_1 ($E_1 \ll E_0$) [30], equations above can be combined to get:

$$f_E = (\nabla \varepsilon \cdot E_0 + \varepsilon \nabla \cdot E_1) E_0 - \frac{1}{2} E_0^2 \nabla \varepsilon \dots\dots\dots(6)$$

The charge conservation equation is [30], $\frac{\partial \rho_q}{\partial t} + \nabla \cdot (\rho_q u) + \nabla \cdot (\sigma E) = 0$, and, $\nabla \times E = 0$

Implied by a very small Reynolds number, the ratio of magnitude of the convection current $\rho_q u$ to the conduction current σE is negligible. Hence the second term in charge conservation equation is omitted. If we consider the field is time varying [30] ($E_0 = \text{Re}[E_0 e^{j\omega t}]$),

We can rearrange the charge conservation equation and get [30],

$$\nabla \cdot E_1 = \frac{-(\nabla \sigma + j\omega \nabla \varepsilon) \cdot E_0}{\sigma + j\omega \varepsilon} \dots\dots\dots(7)$$

The perturbation expansion can be understood as follows. Since field is oscillating with frequency, the steady component of the force produces a continuous motion. For the isothermal case, the total force is zero since there is no free charge. When non-uniform electric fields is present, the heating process produces gradients in local conductivity and

permittivity by $\nabla \varepsilon = \left(\frac{\partial \varepsilon}{\partial T}\right)\nabla T$ and $\nabla \sigma = \left(\frac{\partial \sigma}{\partial T}\right)\nabla T$, leading to the migration of free space charges under electric field and exerting force on fluid through viscosity. Thus, by substituting Equation (7) into Equation (6), we have the final form of the time average electric thermal force [30]:

$$\langle F_{et} \rangle = -0.5 \left[\left(\frac{\nabla \sigma}{\sigma} - \frac{\nabla \varepsilon}{\varepsilon} \right) E \frac{\varepsilon E}{1 + (\omega\tau)^2} + 0.5 |E|^2 \nabla \varepsilon \right] \dots\dots\dots(8)$$

where $\tau = \varepsilon/\sigma$ is charge relaxation time. The formula shows that the thermal force F_{et} follows the directions of electric field and is proportional to the temperature gradient. In aqueous solutions at 293K, we have [22]

$$\frac{1}{\varepsilon} \frac{\partial \varepsilon}{\partial T} = -0.004 \Rightarrow \frac{\nabla \varepsilon}{\varepsilon} = \frac{1}{\varepsilon} \frac{\partial \varepsilon}{\partial T} \nabla T = -0.004 \nabla T / ^\circ C \dots\dots\dots(9)$$

And

$$\frac{1}{\sigma} \frac{\partial \sigma}{\partial T} = 0.02 \Rightarrow \frac{\nabla \sigma}{\sigma} = \frac{1}{\sigma} \frac{\partial \sigma}{\partial T} \nabla T = 0.02 \nabla T / ^\circ C \dots\dots\dots(10)$$

Equation (9) and Equation (10) show that two terms in ACET force have different signs.

By putting the values of equation(9) and Equation (10), we can rewrite the time average electric thermal force as [14]:

$$\langle F_{et} \rangle = -0.5 \varepsilon \left(0.024 \nabla T \cdot E \frac{E}{1 + (\omega\tau)^2} - 0.002 \cdot |E|^2 \cdot \nabla T \right) \dots\dots\dots(11)$$

Letting two terms equal, we can have the crossover frequency $f_c = \frac{\sqrt{11}\sigma}{2\pi\varepsilon}$, which is only dependent on the fluid properties and typically at the range of kHz to Mhz. [23] showed that the Electrothermal force has its maximum effects in a frequency range below the crossover frequency where the Coulomb force dominates.

Chapter 4

Modeling

The modeling of geometry is of two type 2-D and 3-D. First we designed the 2-D geometry of rectangular microchannel with electrode on the sidewalls to find out suitable design parameters, switching patterns of electrodes etc. Then we continue the same on Y- shaped microchannel for mixing fluids of different concentration by integrating the convection diffusion equation. Finally we designed Y-shaped 3-D geometry and continue to study simulation for mixing with various parameters.

In this section, we discuss Geometry design, Fluidic flow pattern and Boundary condition, COMSOL Physics used for simulation and Electrode actuation patterns.

4.1 Geometry (2-D)

The ACET micromixer 2D simulation was carried out using Rectangular and Y-shaped geometry. The Rectangular microchannel of $180 \mu m \times 60 \mu m$ dimensions, has two pairs of microelectrodes, $20 \mu m$ in length, integrated at the bottom of the channel. They were equally spaced with a gap of $20 \mu m$ between the pairs and $10 \mu m$ in between the two electrodes.

The Y-shaped microchannel of $60 \mu m$ height and $280 \mu m$ length, has $25 \mu m$ long microelectrodes at the bottom of channel. They were equally spaced with a gap of $30 \mu m$ between the pairs and $5 \mu m$ in between the two electrodes.

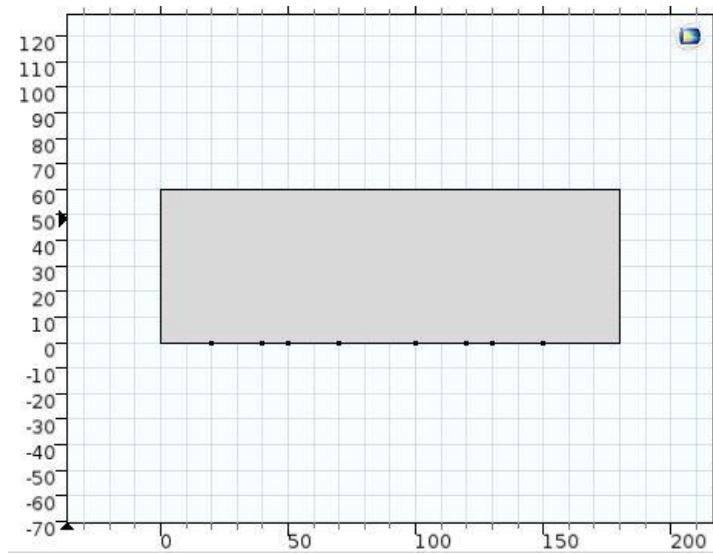


Fig. 2) 2D Rectangular geometry

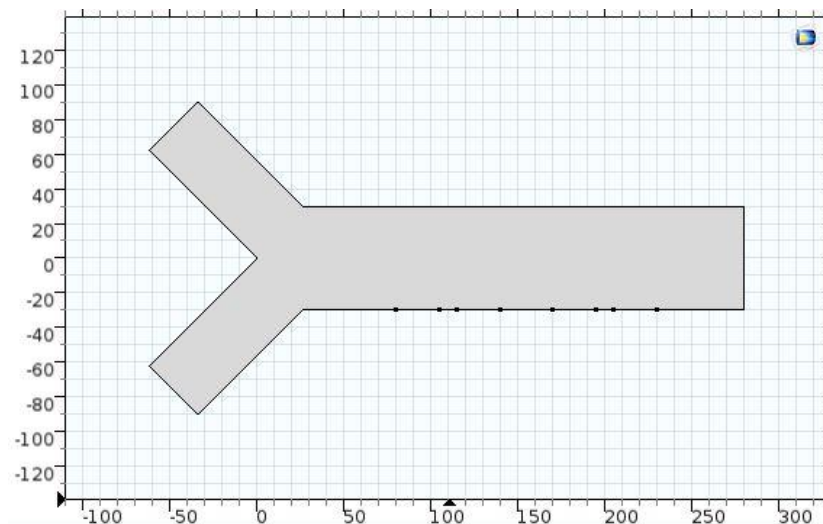


Fig. 3) Y-shaped 2D geometry

4.2 Geometry (3-D)

The 3D simulation was performed using Y-shaped model of $30 \mu m$ in height, $60 \mu m$ width and $280 \mu m$ length. It has 8 microelectrodes of dimension $30 \mu m \times 10 \mu m \times 0.2 \mu m$. They were arranged in two pairs with $20 \mu m$ gap between the pairs and $5 \mu m$ in between the two electrodes.

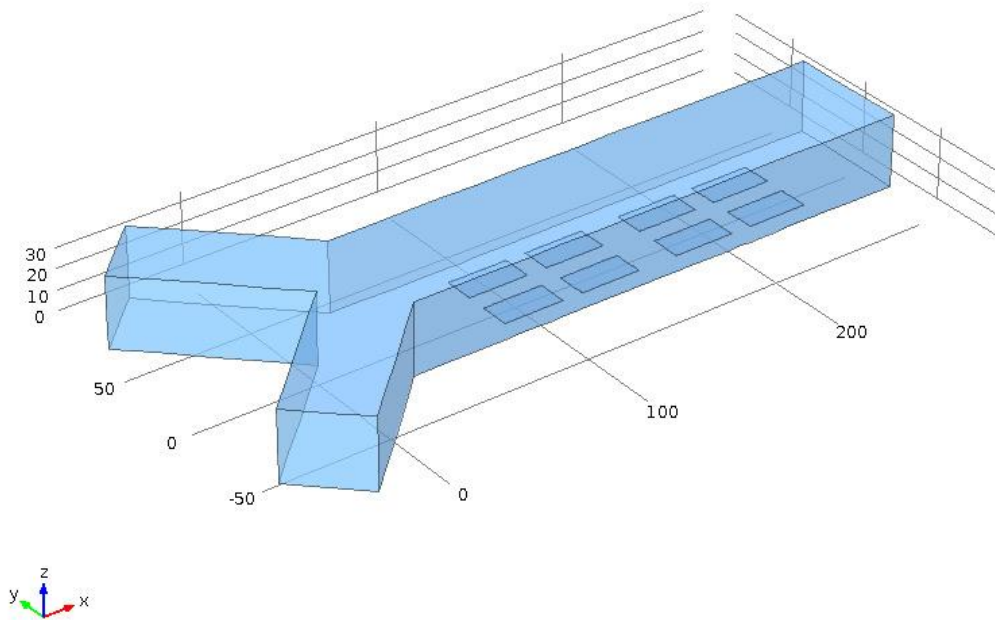


Fig. 4) Y-shaped 3D geometry

4.3 Flow pattern and Boundary condition

Numerical simulation was carried out using COMSOL Multiphysics software. Considering the fluid phase, the model is solved for the coupled electric potential, temperature, and flow fields in two dimensions for simplicity. For this micromixer, a combination of built-in physics simulation modules like Laminar flow, Heat transfer in fluids, Electric current and Transport of diluted species were used. The computational domain comprises one half of the entire microchannel in the horizontal plane due to the symmetry with respect to channel centerline. To solve the coupled electric potential, temperature and flow fields equations, some sets of boundary conditions were imposed to the inlet, channel wall, outlet and channel symmetry.

4.3.1 Laminar flow

Incompressible Navier-Stokes equation with continuity equation was solved.

Inlet and outlet: $n \bullet (\eta \nabla u) = 0$ and $p=0$ i.e the fluids in the end channel reservoirs were assumed to have zero viscous stress and zero pressure(open to air), where n denotes the unit normal vector.

Channel wall: $u=0$ and No slip boundary condition for ACET

Volume force: The electro thermal body force (F_{et}) as given in equation (11)

4.3.2 Heat transfer in fluids

Inlet and outlet: $T= T_0$ ie. The fluids in the end-channel reservoirs were assumed isothermal

Channel wall: $q=-h(T-T_0)$, where q is the outward heat flux due to heat convection with an assumed heat transfer coefficient h.

Total power dissipation density was used as heat source.

4.3.3 Transport of diluted species

Inlet1: incoming fluid of concentration= $0 \text{ mol}/m^3$

Inlet2: incoming fluid of concentration= $1 \text{ mol}/m^3$

Laminar flow velocity was coupled with flow velocity of diluted species.

4.4 Temperature dependent properties

Temperature is the coupling parameter to solve the equations as its affects the fluid properties [2].

$$\sigma(T) = \sigma_0 [1 + \beta(T - T_0)] \dots\dots\dots(12)$$

The above equation shows temperature dependence of fluid electric conductivity, where, σ_0 is the electric conductivity of the fluid at the reference temperature and β is linear temperature coefficient. The values of constants and fluid properties involved in the numerical simulation are listed in the Table below [2].

Name	Value	Unit	Description
T0	293	K	Reference temperature
ϵ_0	$7.10 e^{-10}$	F/m	Fluid permittivity at T0

α	-0.0046	1/K	Temperature coefficient of fluid permittivity
σ_0	0.047	S/m	Fluid electric conductivity at T0
β	0.02	1/K	Temperature coefficient of fluid electric conductivity

4.5 Parameter and Meshing

The 2D geometry was meshed with triangular element meshes using the free mesh parameters tool bar. It is mostly denser near to the boundaries where electrodes are placed. The whole 2D rectangular microchannel geometry contains around 5115 elements. The whole 2D Y-shaped microchannel geometry contains around 17799 triangular elements the complete mesh has 18392 elements. The 3D Y-shaped microchannel geometry contains 135074 tetrahedral elements and 26214 triangular elements, in all 161288 elements.

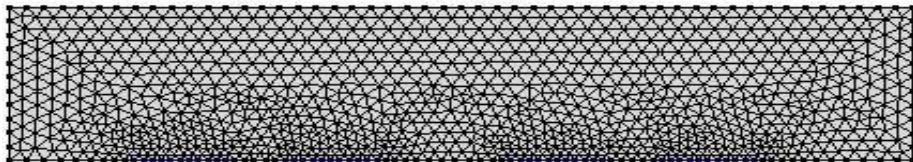


Fig. 5) Rectangular shaped 2D geometry mesh

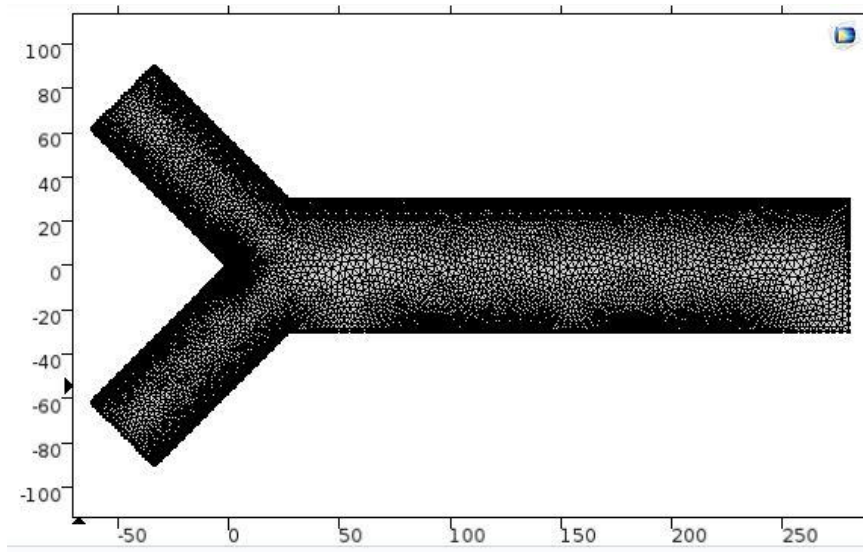


Fig. 6) Y-shaped 2D geometry mesh

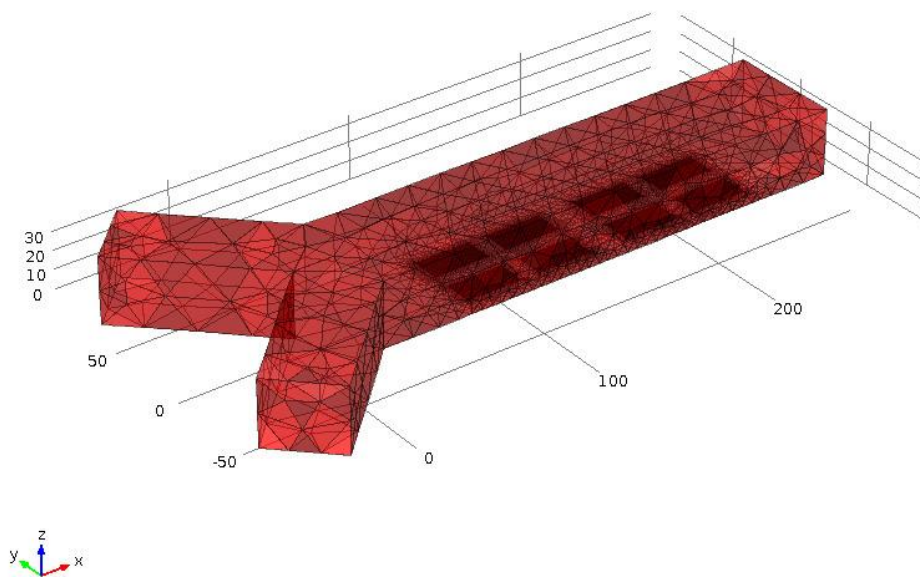
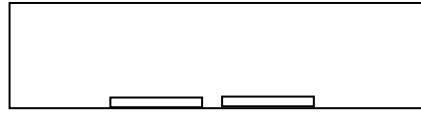


Fig. 7) Y-shaped 3D geometry mesh

4.6 Electrode Actuation Pattern

❖ For 2D simulations different electrode actuation patterns can be as:



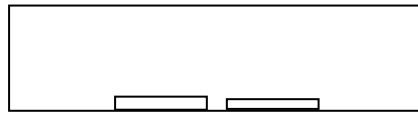
+V -V

a) Two-phase signal with same electrode length



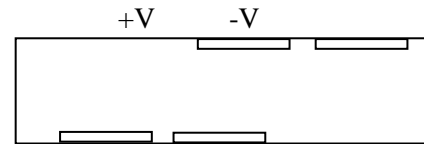
+V -V

b) Two-phase signal with varying electrode length



+V 0V

c) One-phase signal with same electrode length

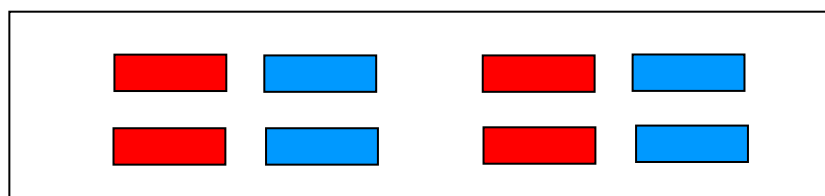


+V -V

d) Two-phases signal with double sided electrodes

A two-phase actuation voltage has shown a 50% increase in the ACET flow rates compared to a single-phase system [34]. When compared to single-phase system, the temperature rise in two-phase system is more because of alternate electric field. This temperature rise with enhanced electric fields results in a larger electric force, which, in turn, leads to a faster fluid flow in the two-phase structure [37]. So in 2D simulations, the electrodes are alternately switched by applying Two-phase AC sinusoidal voltages.

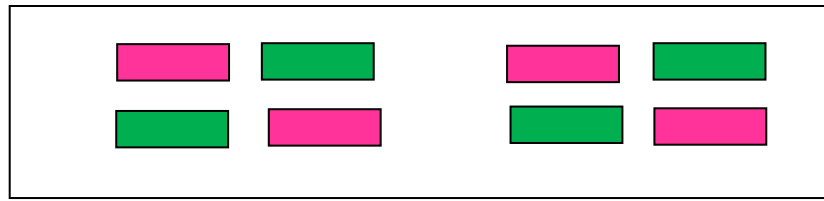
❖ For 3D simulations different electrode actuation patterns can be as:



+Vsin(ωt)

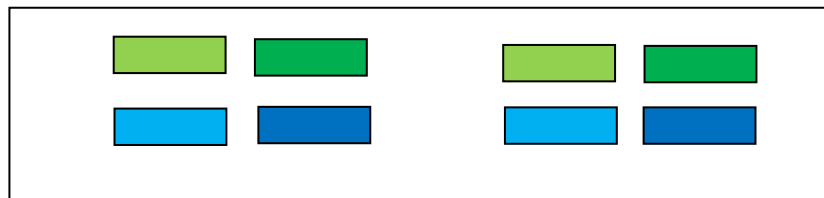
-Vsin(ωt)

Type-a) Two-phase alternate switching of electrodes



$+V\sin(\omega t)$
 $-V\sin(\omega t)$

Type-b) Two-phase crosswise switching of electrodes



$+V\cos(\omega t)$
 $-V\sin(\omega t)$
 $+V\sin(\omega t)$
 $-V\cos(\omega t)$

Type-c) Four-phase crosswise switching of electrodes

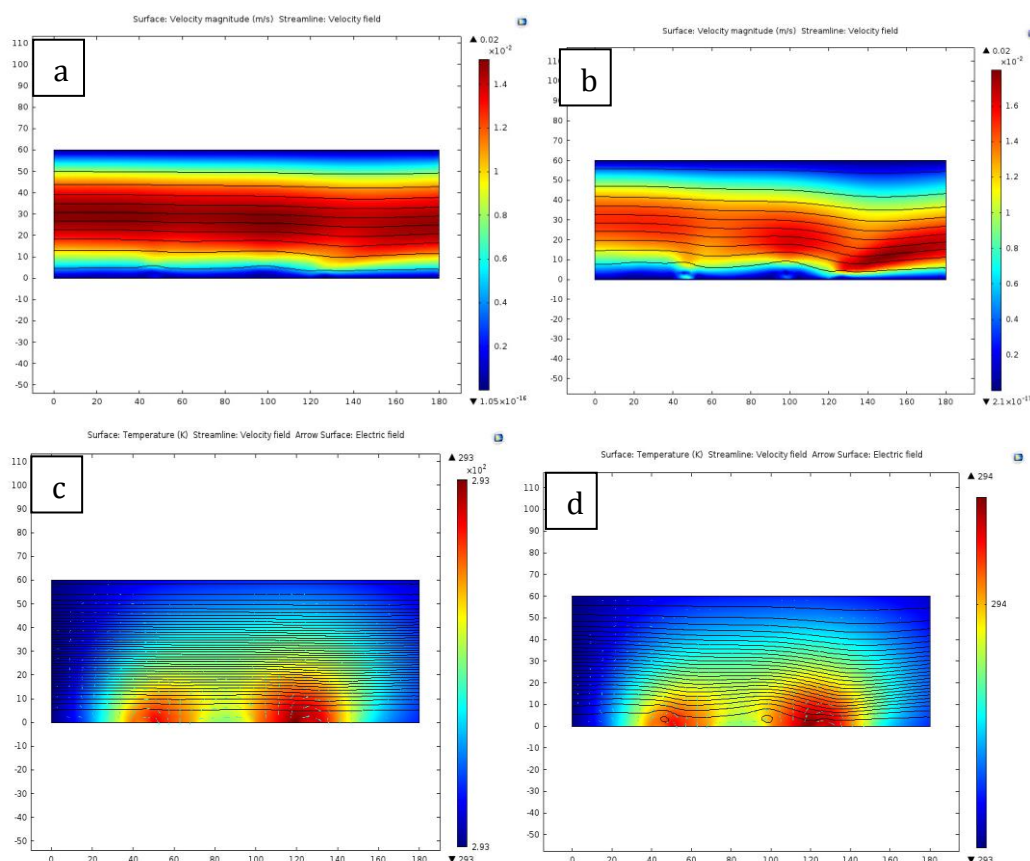
The efficient switching mechanism is required for mixing number of fluids. Out of the above switching patterns, Two-phase crosswise switching has shown comparatively better results. Further 3D simulations were carried out using type-b) switching.

Chapter 5

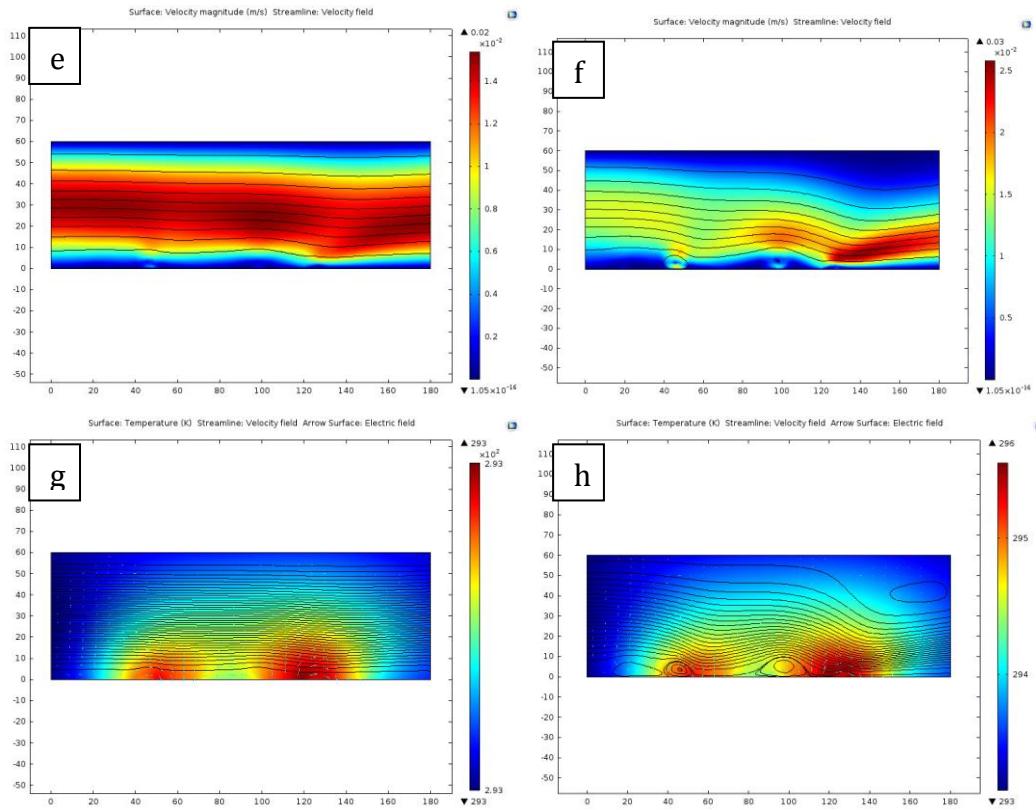
Results and Discussion

5.1 2D Simulation

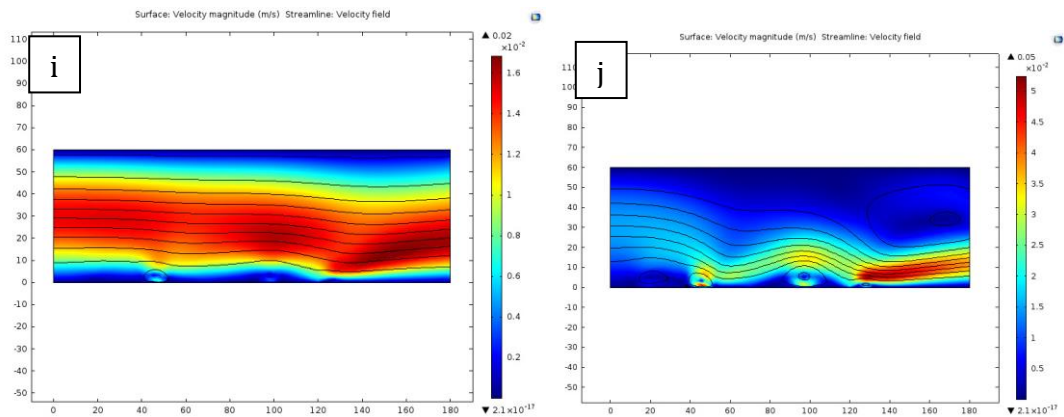
Fig shows the 2D comparison of change in velocity profiles and Temperature profiles with increase in the actuation voltages. Left hand side images corresponds to fluid with $\sigma = 0.001$ s/m and right hand side images corresponds to fluid with $\sigma = 0.01$ s/m. The color variation shows magnitude of velocity at that location with the streamlines at 5V for $\sigma = 0.001$ s/m, the velocity profile is almost parabolic i.e. the fluid has maximum velocity at the centre and minimum near the walls. As the voltages increases, asymmetric flow vortexes can be seen near to electrodes. Significant changes in velocity profile was recorded for $\sigma = 0.01$ s/m fluid at 10V, 100kHz with the temperature change of 293-294 K.

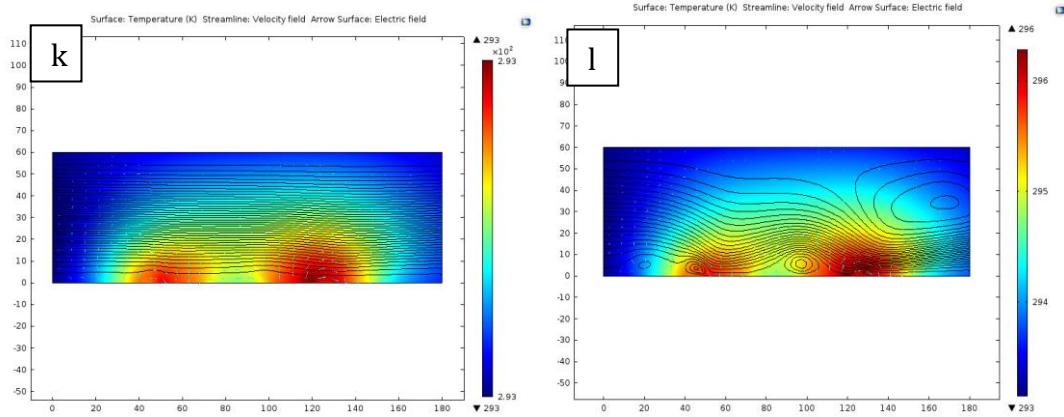


Fig(a)and(b) Velocity profiles of fluid with $\sigma = 0.001$ s/m and $\sigma = 0.01$ s/m at 5V respectively. Fig(c)and(d) Temperature profiles of fluid with $\sigma = 0.001$ s/m and $\sigma = 0.01$ s/m at 5V respectively.

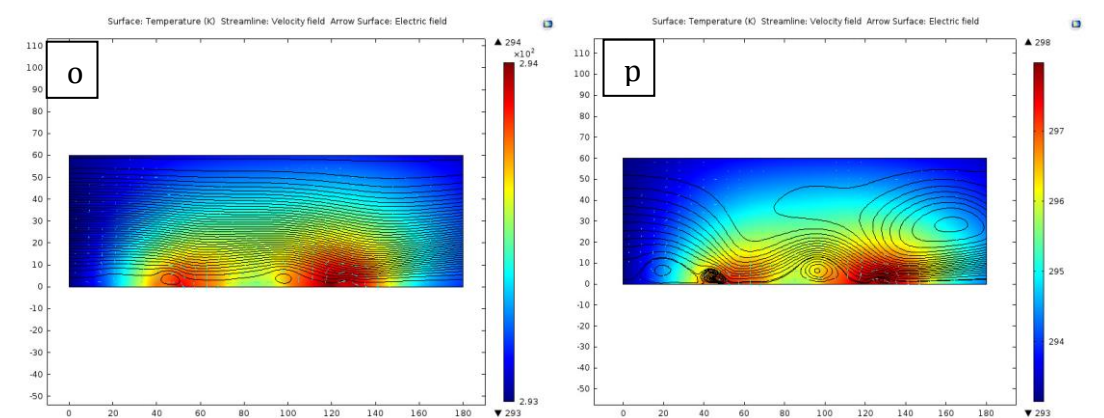
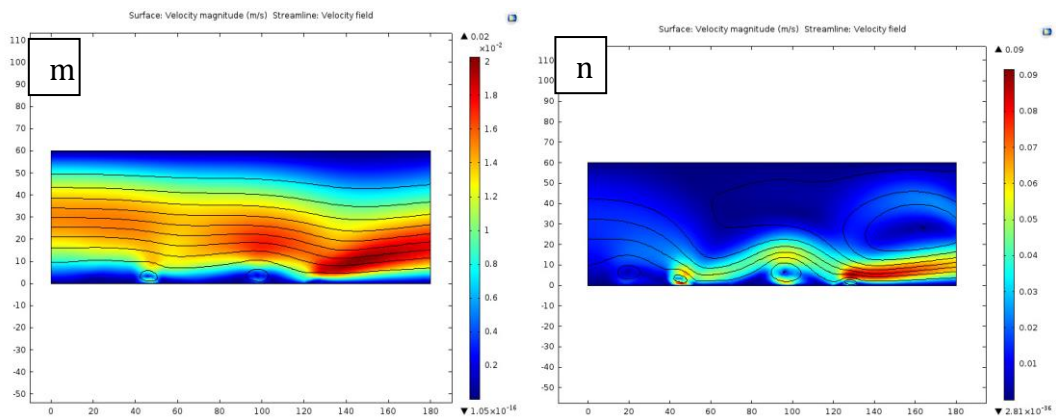


Fig(e)and(f) Velocity profiles of fluid with $\sigma=0.001$ s/m and $\sigma=0.01$ s/m at 7V respectively. Fig(g)and(h) Temperature profiles of fluid with $\sigma=0.001$ s/m and $\sigma=0.01$ s/m at 7V respectively.





Fig(i)and(j) Velocity profiles of fluid with $\sigma=0.001$ s/m and $\sigma=0.01$ s/m at 8V respectively. Fig(k)and(l) Temperature profiles of fluid with $\sigma=0.001$ s/m and $\sigma=0.01$ s/m at 8V respectively.



Fig(m)and(n) Velocity profiles of fluid with $\sigma=0.001$ s/m and $\sigma=0.01$ s/m at 10V respectively. Fig(o)and(p) Temperature profiles of fluid with $\sigma=0.001$ s/m and $\sigma=0.01$ s/m at 10V respectively.

In order to further investigate the fluid velocity dependence on fluid conductivity, the simulations are carried out with fluid of conductivities $\sigma=0.047$ s/m, $\sigma=0.088$ s/m, $\sigma=0.129$ s/m, $\sigma=0.17$ s/m and $\sigma=0.211$ s/m keeping the actuating voltage constant at 10V, 100kHz. Following figures shows that ACET flow velocity increases with increase in conductivity for same applied voltage. The color bar shows velocity magnitude at the colored surfaces. Increase in velocity magnitude from 14mm/s to 0.14m/s. Thus for high conductive fluids by applying small voltages, the temperature gradient increases linearly with conductivity this enhances the electrothermal micromixing.

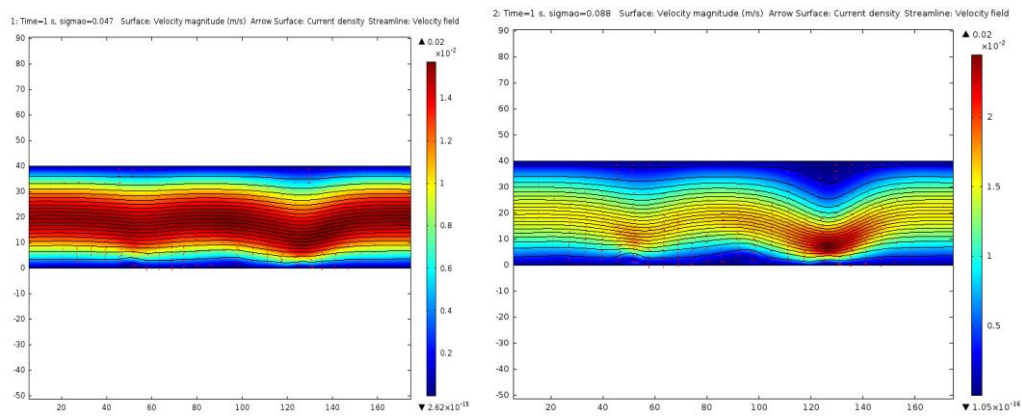


Fig.8) Velocity profiles with velocity magnitude bar for $\sigma=0.047$ s/m, $\sigma=0.088$ s/m fluids.

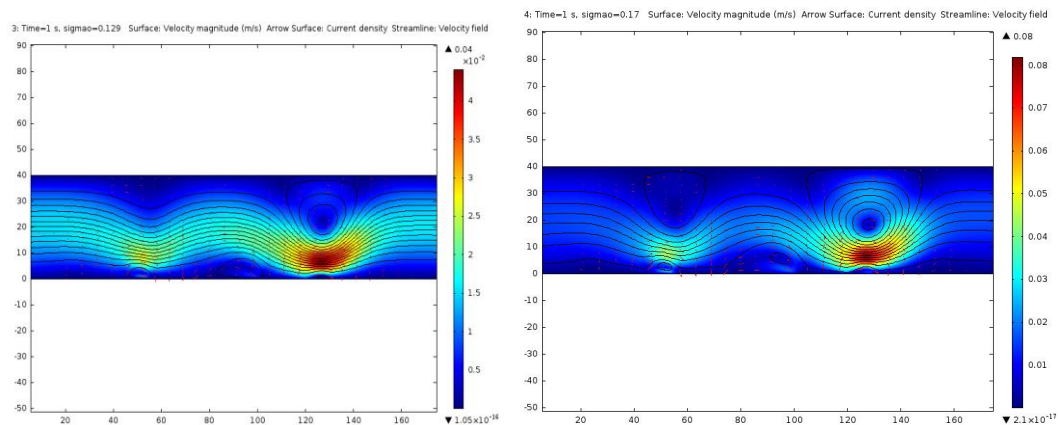


Fig.9) Velocity profiles with velocity magnitude bar for $\sigma=0.129$ s/m, $\sigma=0.17$ s/m fluids.

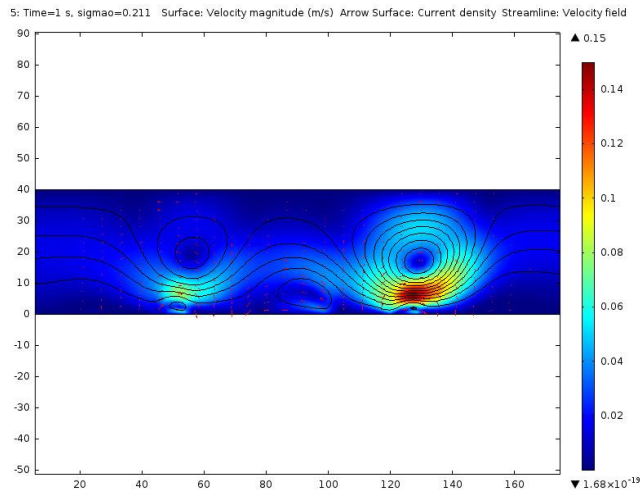


Fig.10) Velocity profiles with velocity magnitude bar for $\sigma = 0.211$ s/m fluid.

In order to further investigate the mixing efficiency, the simulations are carried out in Y-shaped microchannel with two fluids having concentrations of 0 and 1 mol/m^3 at the two inlets. In case of proper mixing, fluid concentration 0.5 mol/m^3 must be obtained at the outlets. Following figures shows the concentration profiles with corresponding applied voltages at different conductivities. Fig shows improved mixing at the outlet for $\sigma = 0.047$ s/m fluid at 8V as compared to $\sigma = 0.01$ s/m fluid at 10V. proper mixing is obtained for $\sigma = 0.1$ s/m fluid at comparatively low voltage of 7V. this simulation shows mixing can be accomplished in a short period of time using ACET flow rather than by diffusion mechanism.

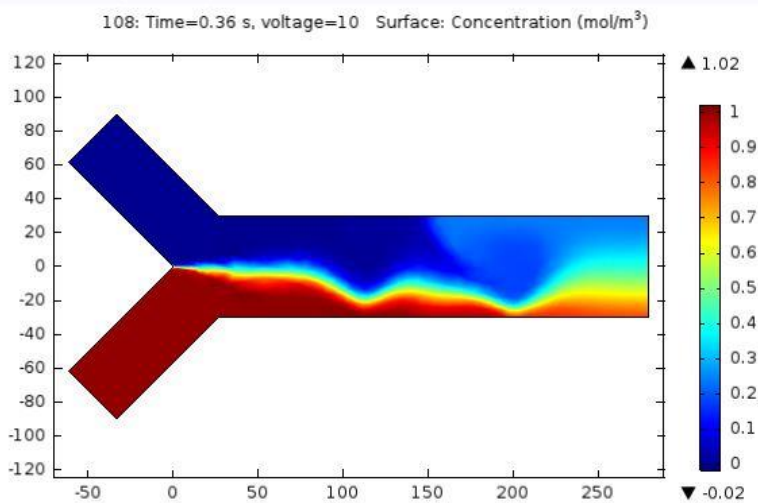


Fig.11) Concentration profile with concentration bar for $\sigma = 0.01$ s/m fluid at $V = 10V$

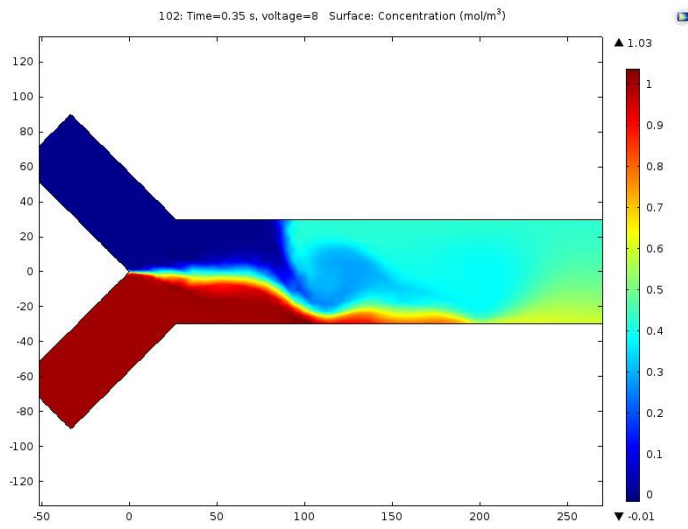


Fig.12) Concentration profile with concentration bar for $\sigma=0.047$ s/m fluid at V=8V

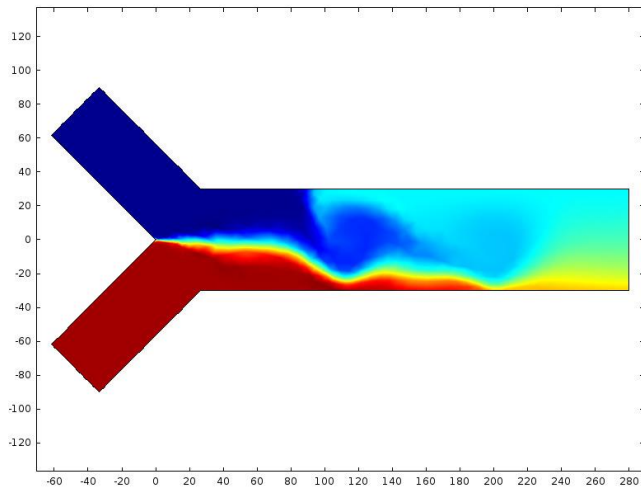


Fig.13) Concentration profile with concentration bar for $\sigma=0.056$ s/m fluid at V=7V

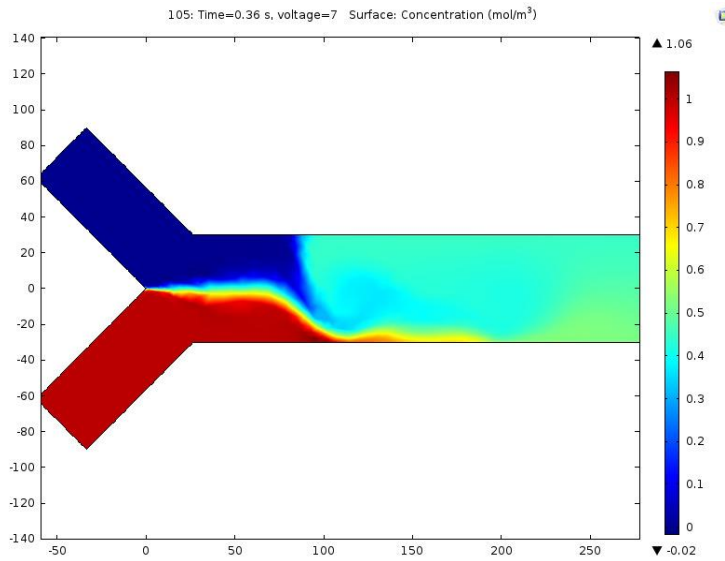
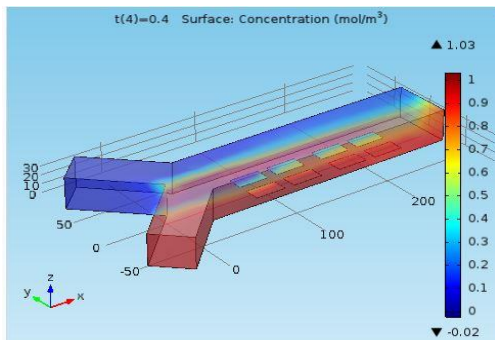


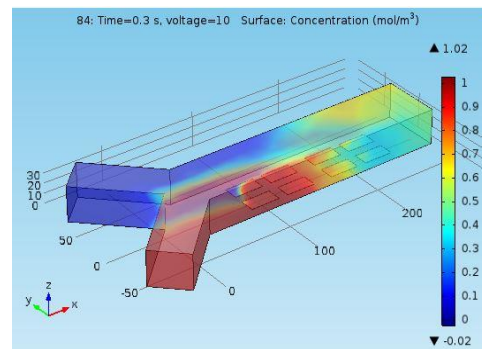
Fig.14) Concentration profile with concentration bar for $\sigma=0.1$ s/m fluid at $V=7V$

5.2 3D simulation

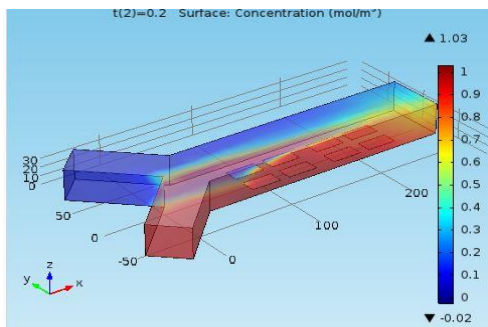
Following figures shows 3D simulation of $\sigma= 0.156$ s/m fluid with three different electrode actuation patterns for mixing as type-a) Two-phase alternate switching of electrodes, Type-b) Two-phase crosswise switching of electrodes, Type-c) Four-phase crosswise switching of electrodes.



Type (a) 2 phase alternate switching for $\sigma= 0.156$ s/m at 10 V



Type (b) 2 phase crosswise switching for $\sigma= 0.156$ s/m at 10 V

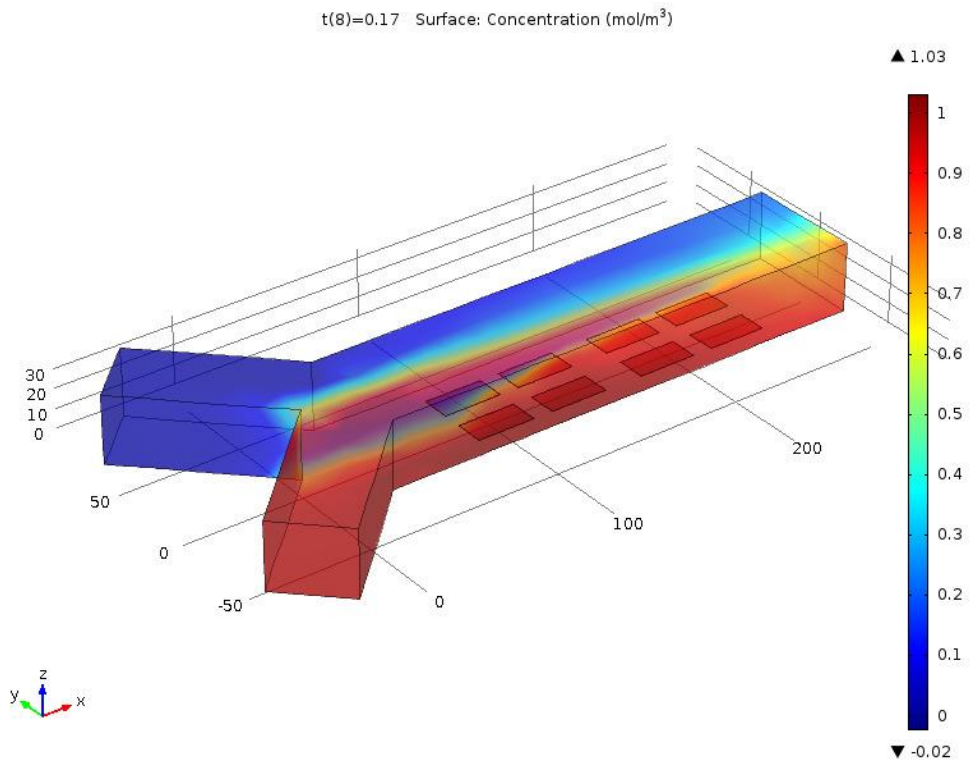


Type (c) 4 phase crosswise switching

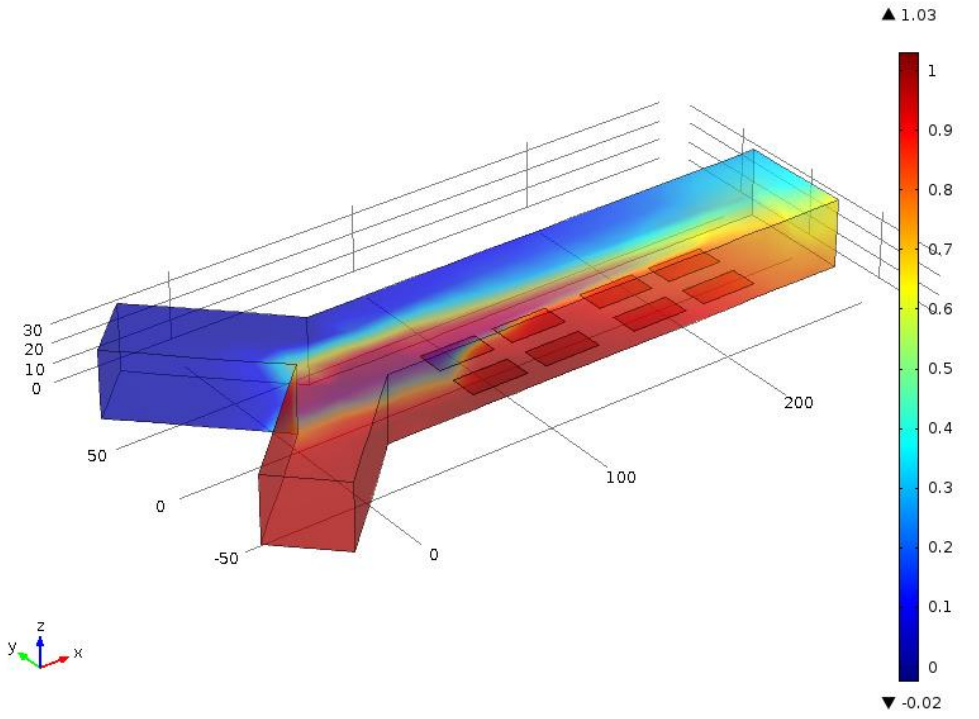
For $\sigma = 0.156$ s/m at 10 V

Out of these switching patterns, Two-phase crosswise switching has shown comparatively better results. A two-phase actuation voltage has shown a 50% increase in the ACET flow rates compared to a single-phase system [34]. Further 3D simulations were carried out using Type (b) switching.

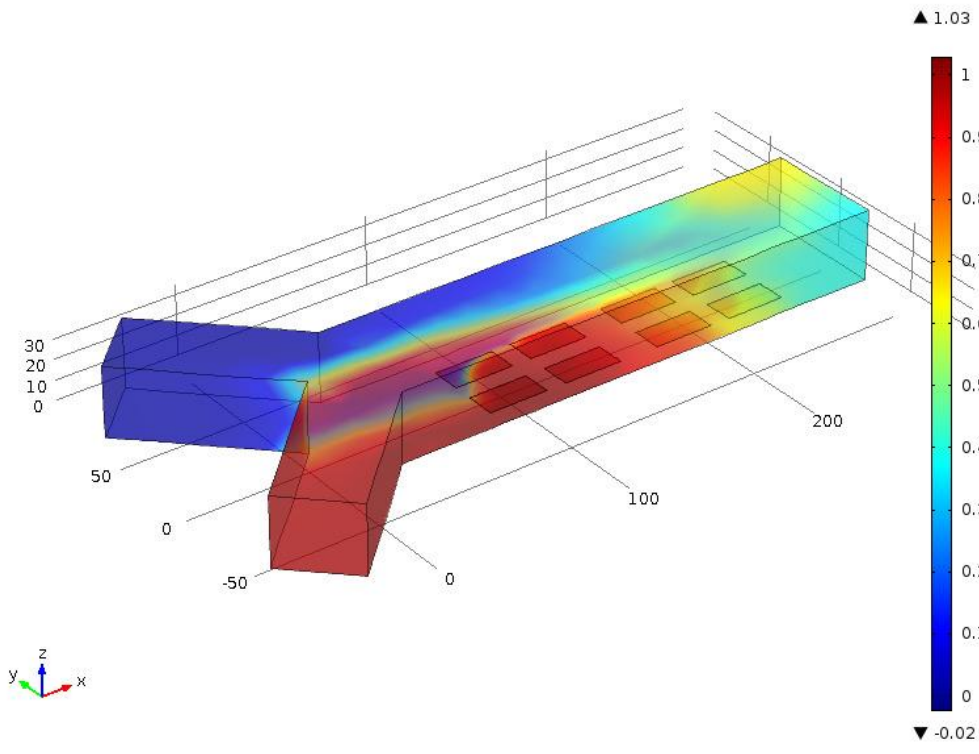
Figure shows 3D simulation step wise results of surface concentration profile for mixing of $\sigma = 0.1$ s/m fluid at 10 V at a particular instant of time. Proper mixing is observed at $t=0.4$ sec.



t(12)=0.21 Surface: Concentration (mol/m³)



t(22)=0.31 Surface: Concentration (mol/m³)



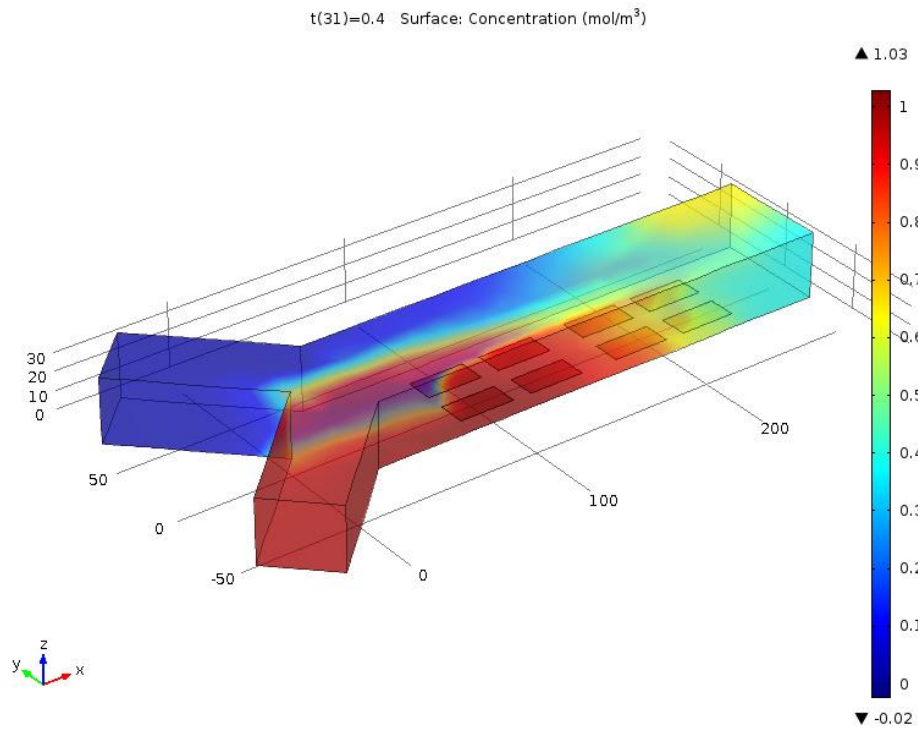


Fig. 15) 3D surface concentration profile with concentration bar for mixing of $\sigma = 0.1$ s/m fluid at 10 V

Comparing 2D simulation results of concentration profiles for $\sigma = 0.1$ s/m fluid with 3D simulation results for the same $\sigma = 0.1$ s/m fluid. It can be seen that in 2D simulation proper mixing was achieved at $V = 7V$, but in 3D proper mixing was achieved at $V = 10V$ as shown above. This contradicts 3D results, this is because 3D simulations are performed by applying the boundary conditions considering the similar experimental conditions at microchannel wall, inlet, outlet, which directly affects simulation results. 3D model simulations have shown optimized flow measurement creating more accurate estimation than 2D model simulations. Biochemical analysis frequently involves samples with high conductivities ie in 0.02-1 s/m range. we have measured fluid velocities around 2.2mm/s for electrothermal flow induced by Joule heating at voltage amplitudes of 9-16V with a range of fluid conductivity from 0.01-0.1S/m. These 3D simulation data/results can be used to fabricate the micromixer and to carry out further experimental analysis.

Here are the list of simulation results with fluid conductivity $\sigma= 0.01$ s/m, $\sigma= 0.1$ s/m, $\sigma= 0.156$ s/m with actuation voltage at different instance of time to optimize mixing at a particular voltage.

1) Difference between maximum and minimum concentration recorded at the end of channel for $\sigma= 0.01$ s/m fluid as shown in table (1):

Table (1)

Time(s)	14V	15V	16V	17V
0.1	0.93	0.92	0.91	0.9
0.2	0.76	0.68	0.55	0.53
0.3	0.65	0.59	0.41	0.22
0.4	0.62	0.45	0.3	0.1

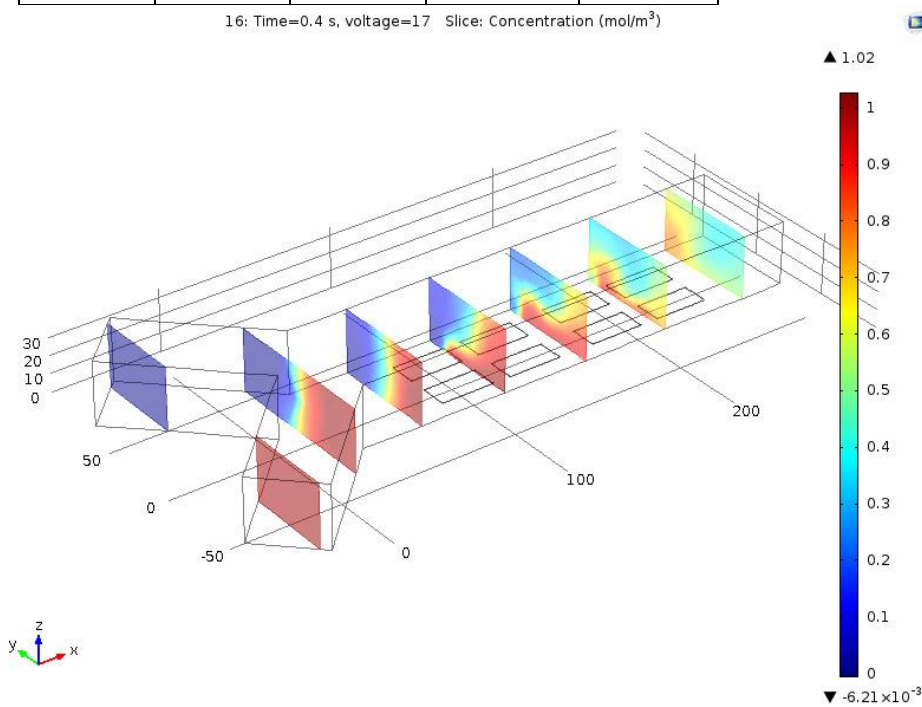


Fig. 16) 3D surface concentration profile with concentration bar for mixing of $\sigma= 0.01$ s/m fluid at 17 V, at 0.4 sec.

2) Difference between maximum and minimum concentration recorded at the end of channel for $\sigma=0.1$ s/m fluid as shown in table (2):

Table (2)

Time(s)	7V	8V	9V	10V
0.17	0.95	0.91	0.89	0.81
0.21	0.81	0.75	0.64	0.52
0.31	0.66	0.54	0.3	0.1
0.4	0.5	0.42	0.21	0.08

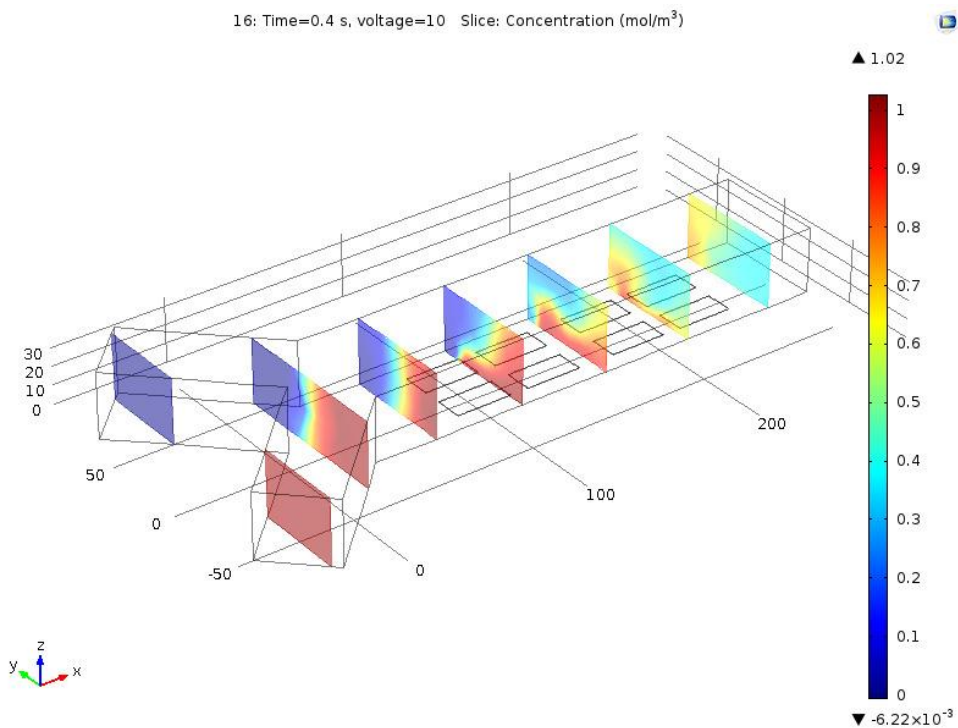


Fig. 17) 3D surface concentration profile with concentration bar for mixing of $\sigma=0.1$ s/m fluid at 10 V, at 0.4 sec

3) Difference between maximum and minimum concentration recorded at the end of channel for $\sigma = 0.156$ s/m fluid as shown in table (3):

Table (3)

Time(s)	7V	8V	9V	10V
0.1	0.86	0.81	0.76	0.68
0.22	0.56	0.52	0.38	0.35
0.31	0.4	0.35	0.09	0.03

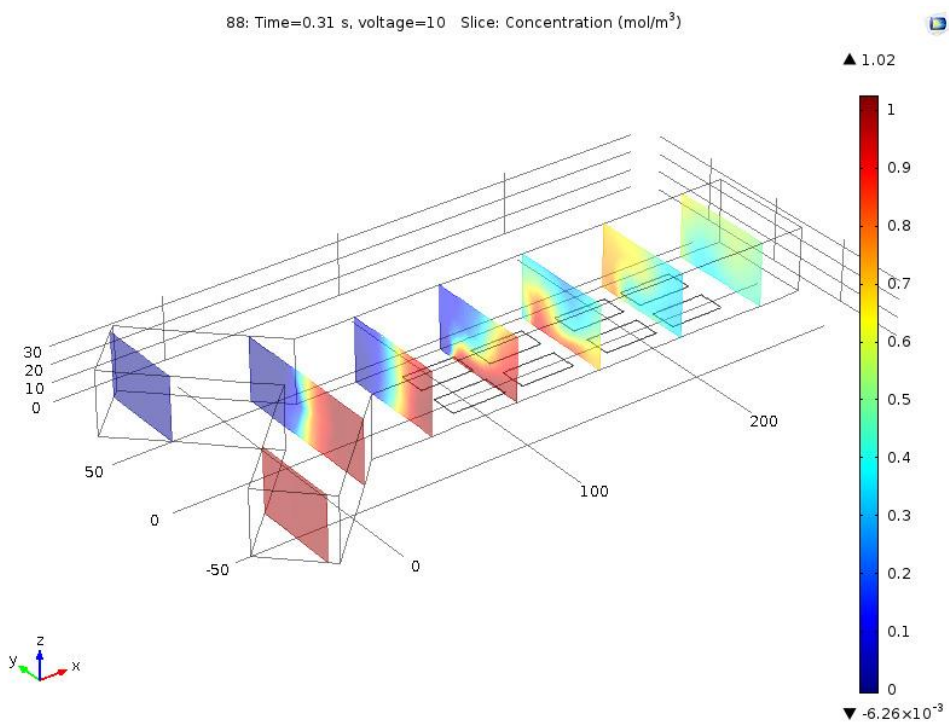


Fig. 18) 3D surface concentration profile with concentration bar for mixing of $\sigma = 0.156$ s/m fluid at 10 V, at 0.31 sec

The above are three optimized micromixer design that can be used in biochemical analysis, detection and measurements.

Conclusion

In the present work, we have simulated 2-D and 3-D mixing geometrical models to study the effect of actuation voltage and electrode switching pattern on flow velocity, temperature and concentration fields. The simulation shows that mixing can be effected in a very short period of time compared with diffusion-based mixing. The two-phase crosswise electrode switching mechanism has shown comparatively better results than single-phase and/or two phase alternate switching. In addition, we have compared the 2-D and 3-D mixing simulation results of fluid $\sigma=0.1$ s/m with respect to time and found that 3D simulations are more accurate and reliable than 2D simulations. Since, 3D simulations were performed considering experimental boundary conditions at microchannel wall, inlet, outlet, which directly affects simulation results. Using the information gathered from the above simulation, the complex systems can be over simplified to address the challenges we mention in this paper.

The LoC does not involve with animal testing and human trial for pharmaceutical research which makes the process cost effective and time saving as well. The idea of home health care device can be extended for applications like RBC count for cancer patient. This emerging technology combines electronics with biology to open new application areas such as point-of-care diagnosis, on-chip DNA analysis, and automated drug discovery.

References

- [1] A. GONZ ALEZ, A. RAMOS, H. MORGAN, N. G. GREEN AND A. CASTELLANOS, "Electrothermal flows generated by alternating and rotating electric fields in Microsystems," J. Fluid Mech. (2006), vol. 564, pp. 415–433.

- [2] S Loire, P Kauffmann, I Mezić and C D Meinhart, “A theoretical and experimental study of ac electrothermal flows,” *J. Phys. D: Appl. Phys.* 45 (2012) 185301 (7pp)
- [3] Oosterbroek, E. and A.v.d. Berg, “Lab-on-a-Chip: Miniaturized systems for (bio)chemical analysis and synthesis,” Elsevier Science. 2nd ed2003
- [4] A. Eden, M. Sigurdson, C. D. Meinhart, I. Mezić, “Numerical Optimization Strategy for Determining 3D Flow Fields in Microfluidics,” 2015 COMSOL Conference in Boston
- [5] Chieh-Li Chen, Her-Terng Yau, Ching-Chang Cho, Cha'o-Kuang Chen, “Enhancement of microfluidic mixing using harmonic and chaotic electric fields,” *International Journal of Nonlinear Sciences and Numerical Simulation*. Vol 10, Issue 11-12, Pages 1545–1554
- [6] Hope C. Feldman, Marin Sigurdson and Carl D. Meinhart, “AC electrothermal enhancement of heterogeneous assays in microfluidics,” *Lab-Chip*, 2007, 7, 1553-1559
- [7] J. J. Feng, S. Krishnamoorthy and S. Sundaram, “Numerical and Analytical Studies of Electrothermally Induced Flow And Its Application For Mixing and Cleaning in Microfluidic Systems,” *NSTI-Nanotech 2004*, ISBN 0-9728422-8-4 Vol. 2, 2004
- [8] Mandy L.Y. Sin, Vincent Gau, Joseph C. Liao, and Pak Kin Wong, “ Electrothermal Fluid manipulation of High-Conductivity Samples for Laboratory Automation Applications,” *JALA* December 2010
- [9] Jonghyun Oh, Robert Hart, Jorge Capurro and Hongseok (Moses) Noh, “Comprehensive analysis of particle motion under non-uniform AC electric fields in a microchannel,” *Lab Chip*, 2009, 9, 62–78
- [10] T J. Cao, P. Cheng, F.J.Hong, “ A numerical study of an electrothermal vortex enhanced micromixer,” *Microfluid Nanofluid* (2008) 5:13–21
- [11] M. H. Oddy, J. G. Santiago, and J. C. Mikkelsen, “Electrokinetic Instability Micromixing,” *Anal. Chem.* 2007, 73, 5822-5832

- [12] Chih-kai Yang, Jeng-Shian Chang, Sheng D. Chao, and Kuang-Chong Wu, "Two dimensional simulation on immunoassay for a biosensor with applying electrothermal effect," APPLIED PHYSICS LETTERS 91, 113904 (2007)
- [13] M. Lian, N. Islam and J. Wu, "AC electrothermal manipulation of conductive fluids and particle for lab-chip applications," IET Nanobiotechnol., 2007, 1, (3), pp. 36–42
- [14] A. Salari, M. Navi, and C. Dalton, "AC Electrothermal Micropump for Biofluidic Applications Using Numerous Microelectrode Pairs," 978-1-4799-7525-9/14/2014 IEEE
- [15] E. Dua and Souran Manoochehri, "Microfluidic pumping optimization in microgrooved channel with ac electrothermal actuations," APPLIED PHYSICS LETTERS 96, 034102 (2010)
- [16] Sophie Loire, Paul Kauffmann and Igor Mezić, "Study of AC Electrothermal Fluid Flow Models," 2011 COMSOL Conference in Boston
- [17] F.J. Hong, J. Cao, P. Cheng , "A parametric study of AC electrothermal flow in microchannels with asymmetrical interdigitated electrodes," International Communications in Heat and Mass Transfer 38 (2011) 275–279
- [18] Ho Jun Kim, and Ali Beskok, "Numerical Modeling of Chaotic Mixing in Electroosmotically Stirred Continuous Flow Mixers," Journal of Heat Transfer, SEPTEMBER 2009, Vol. 131 / 092403-11
- [19] Chun Yee Lim, Yee Cheong Lam, and Chun Yang, "Mixing enhancement in microfluidic channel with a constriction under periodic electro-osmotic flow," Biomicrofluidics 4, 014101-18 (2010)
- [20] Wee Yang Ng, Shireen Goh, Yee Cheong Lam, Chun Yang and Isabel Rodriguez, "DC-biased AC-electroosmotic and AC-electrothermal flow mixing in microchannels," Lab Chip, 2009, 9, 802–809

- [21] David Erickson, David Sinton and Dongqing Li, "Joule heating and heat transfer in poly(dimethylsiloxane) microfluidic systems," *Lab Chip*, 2003, 3, 141–149
- [22] D. R. Lide, "CRC Handbook of chemistry and physics". CRC press," NY, 81st edition, 2000
- [23] D. F. Chen, H. Du, "Simulation studies on electrothermal fluid flow induced in a dielectrophoretic microelectrode system," *Journal of MEMS*, 2006, Vol 16, pp 2411-2419
- [24] Yong Kweon Suh and Sangmo Kang, A Review on Mixing in Microfluidics, *Micromachines* 2010, 1, 82-111
- [25] A. Nisar, N. Afzulpurkar, B. Mahaisavariya, A. Tuantranont, MEMS-based micropumps in drug delivery and biomedical applications, *Sensors and Actuators B*, 2008, 130, pp 917-942
- [26] Bockhorn, H., et al., "Theoretical and Experimental Investigations of Convective Micromixers and Microreactors for Chemical Reactions, in *Micro and Macro Mixing*", D. Mewes and F. Mayinger, Editors. 2010, Springer Berlin Heidelberg. p. 325-346
- [27] Biddiss, E., D. Erickson, and D. Li, "Heterogeneous Surface Charge Enhanced Micromixing for Electrokinetic Flows," *Analytical Chemistry*, 2004. 76(11): p. 3208-3213
- [28] D. Maynes, and B.W. Webb, "Fully-Developed Thermal Transport in Combined Pressure and Electro-osmotically Driven flow in Microchannels" *Journal of Heat Transfer* OCTOBER 2003, Vol. 125 889-895
- [29] M. Sigurdson, D. Wang and C. D Meinhart, "Electrothermal stirring for heterogeneous immunoassays," *Lab-Chip*, 2005, 5, 1366-73
- [30] Ramos A, Morgan H, Green N. G and Castellanos. A, "Ac electrokinetics: A review of forces in microelectrodes," 1998, *J. Phys. D: Appl. Phys* 31, 2338-53

- [31] Sin M L Y, Gau V, Liao J C and Wong P K, "Electrothermal fluid manipulation of high-conductivity samples for laboratory automation applications," 2010, J. Assoc. Laboratory Automation, 15, 426-32
- [32] M. Sigurdson, D. E. Chang, I. Tuval, I. Mezie and C. D. Meinhart, "Ac electrokinetic stirring and focusing of nanoparticles BioMEMS and Biomedical Nanotechnology," 2007 ed M Ferrari et al (New York: Springer) pp 243–5
- [33] Kamholz, A.E., et al., Quantitative Analysis of Molecular Interaction in a Microfluidic Channel: The T-Sensor. Analytical Chemistry, 1999. 71(23): p. 5340-5347
- [34] Rumi Zhang, Colin Dalton, Graham A. Jullien, "Two-phase AC electrothermal fluidic pumping in a coplanar asymmetric electrode array," Microfluid Nanofluid (2011) 10:521–529
- [35] Jie Wu, Meng Lian, and Kai Yang, "Micropumping of biofluids by alternating current electrothermal effects," APPLIED PHYSICS LETTERS 90, 234103 (2007)
- [36] Nazmul Islam, "Enhancing AC Electrothermal Micropumping by Integrating Temperature Bias and Surface Modification," Islam; JSRR, Article no. JSRR.2014.11.004
- [37] Rumi Zhang, Graham A. Jullien, and Colin Dalton, "Study on an alternating current electrothermal micropump for micro-needle based delivery systems," JOURNAL OF APPLIED PHYSICS 114, 024701 (2013)